S.Ü. Müh.-Mim. Fak. Derg., c.27, s.4, 2012
J. Fac.Eng.Arch. Selcuk Univ., v.27, n.4, 2012
ISSN: 1300-5200, ISSN: 1304-8708 (Elektronik)

PREPARATION OF POLYANILINE/ZnO NANOCOMPOSITES BY USING ARC-DISCHARGE SYNTHESIZED ZNO NANOPARTICLES AND PHOTOCATALYTIC APPLICATIONS

Volkan ESKİZEYBEK[1], Handan GÜLCE*[2], Ahmet GÜLCE[3], Ahmet AVCI[4], Eda AKGÜL[5]

[1,4]*Departmet of Mechanical Engineering, Selcuk University, Selcuklu 42075, Konya Turkey*
[2,3,5]*Departmet of Chemical Engineering, Selcuk University, Selcuklu 42075, Konya Turkey*
**Corresponding Author: hgulce@selcuk.edu.tr*
[1]veskizeybek@selcuk.edu.tr, [2]hgulce@selcuk.edu.tr, [3] agulce@selcuk.edu.tr, [4] aavci@selcuk.edu.tr,
[5]tageda@hotmail.com

ABSTRACT: Polyaniline (PANI) and PANI/ZnO nanocomposites were synthesized by the chemical oxidative polymerization of aniline and aniline with the presence of ZnO nanoparticles, respectively. The ZnO nanoparticles synthesized by arc-discharge method were used in this study to produce PANI/ZnO nanocomposites. Aniline/ZnO nanoparticles molar ratio was changed to investigate the effect of ZnO nanoparticles to the characteristic of the PANI. The scanning electron microscope analysis showed that ZnO nanoparticles were completely dispersed in PANI matrix homogeneously. It is revealed that shifting to the higher wavenumbers occurred by the increasing ZnO nanoparticle content in fourier transform infrared spectroscopy analysis. Furthermore, degradation of malachite green in aqueous solution was carried out with the prepared nanocomposites under ultraviolet irradiation. The experimental results showed that 1.2 g/L of the nanocomposite could catalyze green solution above 98% after 180 min of irradiation.

Keywords: *Polyaniline, ZnO, Arc-discharge, Chemical polymerization, Nanocomposite*

Ark-Deşarj Yöntemi ile Sentezlenen ZnO Nanoparçacıkları Kullanılarak Hazırlanan Polianilin/ZnO Nanokompozitleri ve Fotokatalitik Uygulamaları

ÖZET: Polianilin (PANI) ve PANI/ZnO nanokompozitleri, sırasıyla anilin ve ZnO nanoparçacık ilave edilmiş anilinin kimyasal oksidatif polimerizasyonu ile sentezlenmiştir. ZnO nanoparçacıkları ark-deşarj yöntemi ile sentezlenerek PANI/ZnO nanokompozitlerinin hazırlanmasında kullanılmıştır. ZnO nanoparçacıklarının PANI'nin karakteristiği üzerindeki etkisini incelemek amacıyla Anilin/ZnO nanoparçacık molar oranı değiştirilmiştir. Taramalı elektron mikroskopisi analizlerine gore, ZnO nanoparçacıkları PANI matriks içerisinde homojen bir şekilde dağıtılmıştır. PANI/ZnO nanokompozitlerinin Fourier dönüşümlü Infrared spektroskopisi ile yapılan incelemelerinde, PANI matriks içerisindeki ZnO nanoparçacık miktarı arttıkça PANI'ye ait karakteristik bantların daha yüksek dalga boylarına kaydığı tespit edilmiştir. Ayrıca, hazırlanan nanokompozitler ile malahit yeşili sulu boya çözeltisinin ultraviole ışık etkisi altında bozunması araştırılmıştır. Deneysel olarak elde edilen sonuçlara gore, malahit yeşili sulu çözeltisi içerisine 1,2 g/L PANI/ZnO nanokompozit katalizörü katıldığında 180 dakika sonunda %98'in üzerinde bozunma gerçekleştiği bulunmuştur.

Anahtar Kelimeler: *Polianilin, ZnO, Ark-deşarj, Kimyasal polimerasyon, Nanokompozit*

1. INTRODUCTION

Polyaniline (PANI) is one of the promising polymers due to high conductivity, simple synthesis procedure, good environmental stability and reversible acid base chemistry in aqueous solution [Sailor *et al.*, 1990 and Gustafsson *et al.*, 1992] and a large variety applications such as in electro-chromic devices,

light emitting diodes, corrosion-protecting paint and electrostatic discharge protection [Gangpadhyay and De, 2000; Zhang *et al*., 2004; Lee *et al*., 2004]

In recent years, the interest in the development of inorganic/polymer hybrid materials on nanometer scale has grown due to a wide range of potential applications in opto-electronic devices [Zhang *et al*., 2004; Lee *et al*., 2004; Beek *et al*., 2005] and in field effect transistors [Sui *et al*, 2005]. Due to the inorganic fillers at nanoscale exhibit quite different electronic and optical properties from those of their bulk state, it is expected to obtain a new composite material that has synergetic or complementary behaviors between the polymer and inorganic material.

Among inorganic nanoparticles, ZnO is a wide band gap semiconductor (3.37 eV) with a 60 meV exciton binding energy, which permits laser emission at room temperature [Olson *et al*., 2006]. This large band gap is suitable for the use of ZnO to collect high-energy photons (UV light) [Xu *et al*., 2007]. These attractive physical properties give this oxide potential application in optoelectronics [Cho *et al*., 1999; Bae *et al*., 2003; Özgür *et al*., 2005]. Various authors currently obtain ZnO nanorods with diameters of 20–100 nm [Yan *et al*. 2001; Zamfericscu *et al*., 2002; Park *et al*., 2002; Wang *et al*.; Banarjee *et al*., 2005; Yang and Wang, 2005]. Obtaining a large quantity of one-dimensional ZnO nanostructures may allow to study of the optical, photo-catalytically and mechanical properties. There are few studies reporting the synthesis, morphology, optical, electrical and photocatalytical properties of ZnO/PANI nanocomposites [Chang *et al*., 2004; He, 2004; He, 2005; Paul *et al*., 2007; Sharma *et al*., 2009a; Khan and Khalid, 2009; Sharma *et al*., 2009b; Sharma *et al*., 2009c; Ameen *et al*., 2011; Eskizeybek *et al*., 2012].

In this study, we reported the synthesis of PANI/ZnO nanocomposites via oxidative polymerization method in water and the effects of different weight percent of ZnO nanoparticles to the nanocomposite properties. The ZnO nanoparticle synthesized by arc-discharge method was used for the first time in this study to produce PANI/ZnO nanocomposites. The nanocomposites were characterized by using scanning electron microscopy (SEM), X-ray diffraction (XRD) analysis, fourier transform infrared spectroscopy (FTIR), UV-visible spectroscopy (UV-vis), differential scanning calorimetry (DSC) analysis. In addition, photocatalytic activities of the prepared nanocomposites were characterized based on photocatalytic degradation of malachite green in aqueous solution under ultraviolet (UV) light irradiation.

2. MATERIAL AND METHOD

All chemicals used were of analytical reagent grade. Aniline (Merck) was distilled under reduced pressure, stored in dark below 4°C. High purity Zn rods (99.99%) were supplied by Alfa Aesar. Sodium dodecyl sulfate (SDS), ammonium peroxydisulfate (APS) and ethanol (Merck) were used as received. De-ionized water was used to synthesize ZnO nanoparticles. Bi-distilled water was used throughout the experimental work.

Arc-discharge (AD) method submerged in deionized (DI) water was used to synthesize ZnO nanoparticles as reported before [Eskizeybek *et al*., 2011]. The AD apparatus consists of two Zn electrodes as anode and cathode. The AD was initiated in the DI water by touching the anode to the cathode and then the gap between the electrodes was controlled by measuring discharge voltage to achieve maintain stable AD. The applied arc current was kept constant in 50 A for the whole experiment. AD was continued for 3 minutes and after discharging, the solution was kept at room temperature for several days to provide settling of the synthesized particles in the DI water. The settled products and DI water was separated by decantation and then dried at 80°C under vacuum conditions.

PANI was synthesized by polymerization of aniline in water by chemical oxidation. For the synthesis, 0.21 mole aniline and 1.5 mmole SDS were dissolved in 20 mL water. ZnO nanoparticles with different weight percents were added in the aniline solution and were sonicated for 24 h to improve the suspension of ZnO nanoparticle in the solution.

4.3 mmole APS was dissolved in 5 mL water and added by means of drop wise to aniline solution. The solution was mixed for one minute by means of magnetic agitation at room temperature then the polymerization realized in the refrigerator at 4°C for overnight. The polymerization procedure was also realized to synthesize pure PANI without adding ZnO nanoparticles. The resulting greenish black participate was filtered and washed several times with distilled water and ethanol to remove unreacted chemical followed by drying in desiccators under vacuum at room temperature for 24 h. The PANI/ZnO nanocomposites were prepared by adding $28x10^{-5}$ mole, $14x10^{-5}$ mole, $9.0x10^{-5}$ mole and $4.5x10^{-5}$ mole ZnO nanoparticles in polymerization medium and the nanocomposites synthesized in this study were called NC1, NC2, NC3 and NC4 respectively.

X-Rays Diffraction (XRD) analysis was carried out by Shimadzu XRD-6000 X-ray diffractometer using Cu K_α radiation (λ=0.15418 nm) the operating conditions were 40 kV and 30 mA in the scanning range from 20°-70° at rate of 2°/min. SEM images of the synthesized products were carried out using a JEOL/JSM-6335F-EDS SEM. The samples were dissolved in water by ultrasonication and their optical absorption spectra was obtained using an Ocean Optics HR4000 UV-visible spectrophotometer and the FTIR spectra of zinc oxide and polyaniline-zinc oxide composites were recorded by a Perkin Elmer 1725 instrument. The thermogravimetric analysis were performed on the selected samples of composites and polyaniline by using a Perkin–Elmer (Pyris Dimond) instrument heating from 25°C to 600°C at the rate of 10°C min^{-1} in nitrogen atmosphere with the flow rate of 20 mL/min.

The photocatalytic degradation of MG dye was performed in quartz tubes using NC1 and NC4 nanocomposites as catalysts under the illumination of UV light. 2.5 mL $1.0x10^{-6}$ M MG solution was mixed with 3.0 mg catalysts. Before irradiation, suspension was stirred for 30 minutes in dark conditions until adsorption-desorption equilibrium was established. And then the suspensions were irradiated without stirring. The catalytic degradation of MG was investigated at room temperature in the presence/absence of catalyst under irradiation/dark for given times. The concentration of dye in each sample was analyzed by using UV–vis spectroscopy method and absorptions of the MG at characteristic wavelength were measured. The decolorization efficiency of dye is estimated by the following equation;

$$Degradation\ rate\ (\%) = ((A_0-A)/A_0)x100 \quad (1)$$

where A_0 represents the absorbance of dye before illumination, A denotes the absorbance of dye after a certain irradiation time.

3. RESULTS AND DISCUSSIONS

The oxidation of aniline in an acidic aqueous medium yields PANI. When the reaction mixture contains ZnO nanoparticles, nanocomposite materials of both components are obtained. Nanocomposite structures depending on the nature of the components used and the method of preparation. Different polymerizations were carried out in which an aniline concentration was kept constant and different concentrations of ZnO nanoparticles were added to the aniline solution as described in experimental section. The SEM images, FTIR and UV-visible spectra and DSC curves prove that PANI and PANI/ZnO composites have been produced. The characterizations of the ZnO nanoparticles and pure PANI have been studied. The characterizations of nanocomposite materials have also been studied to compare the molecular structures of the nanocomposites, PANI and ZnO nanoparticles.

The XRD and TEM images of ZnO nanoparticles synthesized in the present work using the AD technique are shown in Fig. 1a and b, respectively. The various peaks in the XRD pattern could be assigned to the crystalline zinc oxide phase with the hexagonal wurzite structure with the lattice parameters a=0.324 nm and c=0.519 nm (joined powder diffraction files JPDS No.30-1451). The TEM image exhibits that the ZnO nanoparticles are rod in morphology and 20-100 nm in size. The ZnO nanorods with

different diameters and the agglomerated ZnO nanoparticles can be seen in Fig. 1b.

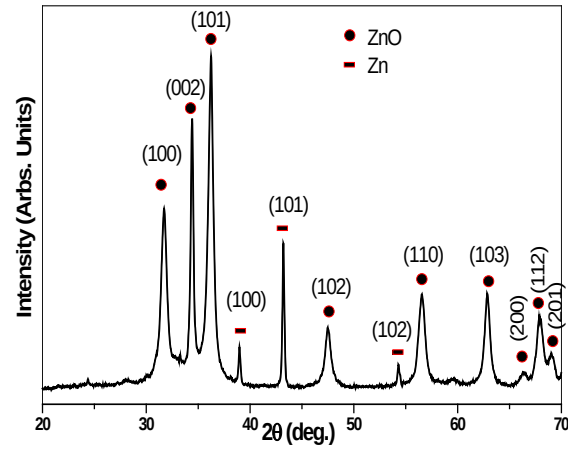

(a)

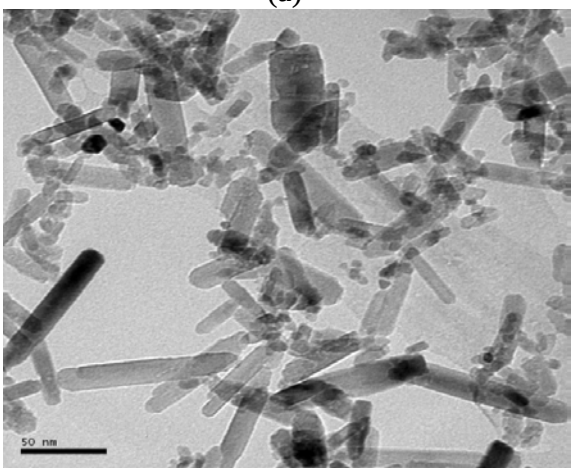

(b)

Figure 1. a) XRD pattern of as synthesized material showing the coexistence of ZnO and zinc phases b) Typical TEM image of the prepared ZnO nanorods shows the presence of small ZnO nanoparticles.

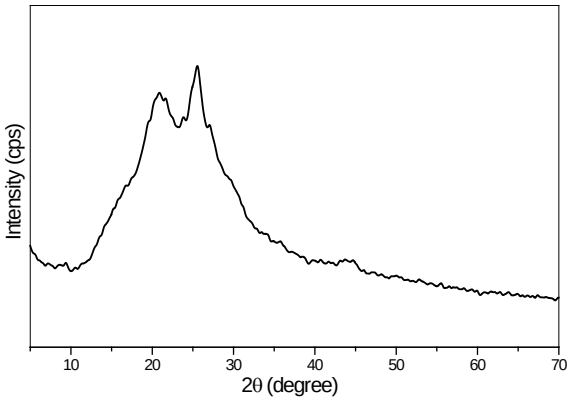

Figure 2. XRD pattern of NC1 nanocomposite

Crystallinity and orientation of conducting polymer have been of interest, because more highly ordered system could display a metal-like conducting state. Fig. 2 represents the XRD pattern of the PANI/ZnO nanocomposite named as NC1. As can be seen in Fig. 2 two peaks centered at 2θ = 21° and 26° are observed in XRD pattern of NC1 sample. The peak centered at 2θ = 21° may be ascribed to periodicity parallel to the polymer chain, while the peak at 2θ = 26° may be due to the periodicity perpendicular to the polymer chain. The peak at 2θ = 21° also represents the characteristic distance between the ring planes of benzene rings in adjacent chains or the close contact inter-chain distance [Pouget *et al.*, 1995]. The peak of 2θ = 26° is stronger than that of 2θ = 21°, due to highly doped emeraldine salt. This result is in good agreement with the reported results in the literature [Singla *et al.*, 2007].

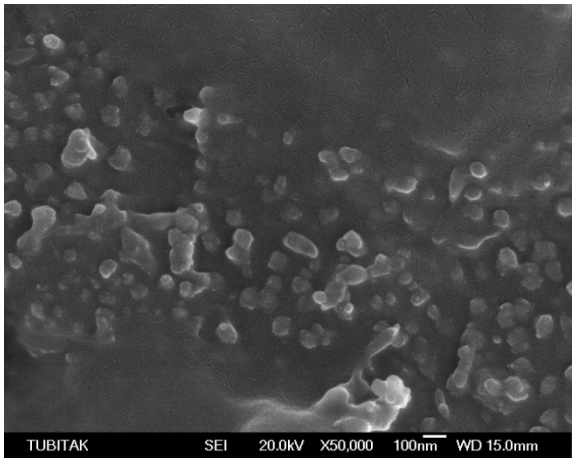

(a)

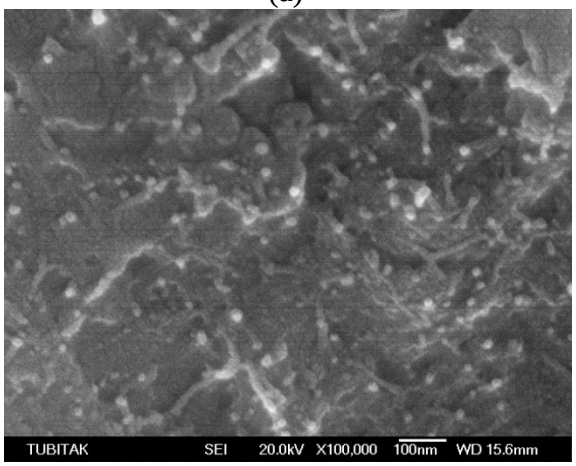

(b)

Figure 3. SEM images of a) PANI homopolymer, b) PANI/ZnO nanocomposites named as NC1.

The SEM images of the synthesized PANI homopolymer and PANI/ZnO composites have been shown in Fig. 3 a and 3b, respectively. As can be seen in Fig. 3a and 3b, the morphology of PANI is amorphous and the ZnO nanoparticles were attached with polyaniline during polymerization. The SEM image of composite shows that there is no agglomeration of ZnO particles in PANI matrix and there is a uniform distribution of the ZnO rods in the PANI matrix.

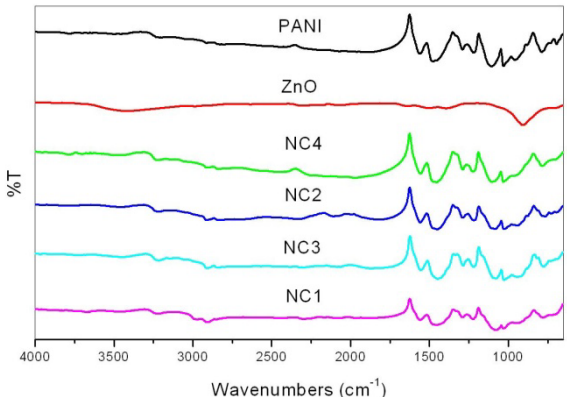

Figure 4. FTIR spectrum of PANI homopolymer, ZnO nanoparticles and PANI/ZnO nanocomposites.

FTIR spectra of ZnO nanoparticles, PANI and PANI/ZnO composites that synthesized by different molar ratio of aniline/ZnO have been shown in Fig. 4, respectively. The characteristic peaks of PANI at 1561 cm^{-1} (C=C stretching mode of the quinoid rings), 1479 cm^{-1} (C=C stretching mode of benzenoid rings), 1287 cm^{-1} (C-N stretching mode of the quinoid rings) and 1100 cm^{-1} (N=Q=N, where Q represents the quinoid ring) appear in the FTIR spectrum of PANI. The PANI/ZnO composites also show the same characteristic peaks. It is evident from Fig. 4 (curve NC1, NC2 NC3, NC4) that the FTIR spectra of the PANI/ZnO composites seem to be a mixture of both ZnO and PANI spectra, showing the formation of polyaniline in the composite. However, the corresponding peaks of pure PANI at 3225 cm^{-1} (N-H stretching mode of benzenoid rings) shifted to 3215 cm^{-1}, 1561 cm^{-1} shifted to 1555 cm^{-1}, 1479 cm^{-1} shifted to 1445 cm^{-1}, 1100 cm^{-1} shifted to 1080 cm^{-1}, 1030 cm^{-1} shifted to 1021 cm^{-1}, 955 cm^{-1} shifted to 943 cm^{-1} and 789 cm^{-1} shifted to 775 cm^{-1} wavenumbers in PANI/ZnO composites, approximately. Comparing to the characteristic peaks of PANI, some of the bands of PANI/ZnO composites shift to the lower wavenumbers, which may be ascribed to the hydrogen bonding action between ZnO nanoparticles and the N-H group in the PANI molecular chains. Such interactions were also reported earlier for PANI/ZnO composites [Sailor *et al*., 1990 and Gustafsson *et al*., 1992; Gangpadhyay and De, 2000; Zhang *et al*., 2004; Lee *et al*., 2004; Beek *et al*., 2005; Sui *et al*, 2005]. These results confirm to presence of ZnO in composite materials. Furthermore, the peak at 1218 cm^{-1}, characteristic of conducting emeraldine salt form of PANI, is also observed at FTIR spectra of PANI and PANI/ZnO composites. It has been interpreted as originated from bipolaron structure related to the C-N stretching vibrations [Pouget *et al*., 1995]. The results indicate that all the polymer and composite materials are in doped state. The peak intensity at 1218 cm^{-1} (C-N stretching mode of bipolaron structure) is higher than the peak that the result of most doped nanocomposite is NC1.

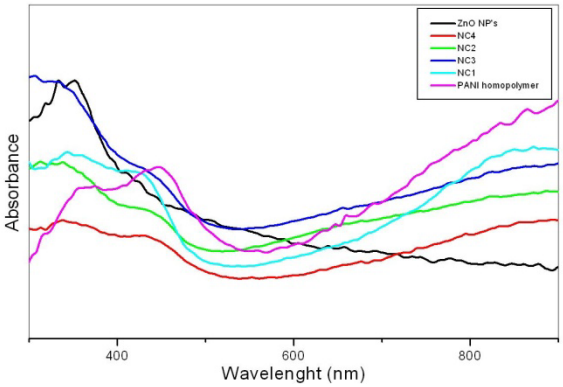

Figure 5. UV-Vis. spectrum of PANI homopolymer, ZnO nanoparticles and PANI/ZnO nanocomposites.

The UV-visible spectra of ZnO, PANI and PANI/ZnO composites with various molar ratios of PANI/ZnO are shown in Fig. 5. PANI shows three absorption bands at 350nm, 450 nm and around 900 nm wavelengths. As reported previously by some researchers doped forms of PANI usually show three characteristic absorption bands at 320-360, 400-450 and 740-950 nm [Wang *et al*., 2010]. The first absorption band

arises from π-π electron transition within benzenoid segments. The second and third absorption bands are related to doping level and formation of polarons (quinoid segments), respectively. For PANI, not completely separated bands seen in 350nm to 450 nm and the band seen at around 900 nm is an indication of high doping level. The absorption band of ZnO at 350 nm overlaps with the absorption band of PANI at the same wavelength value for ZnO/PANI composites. Doping state of each nanocomposite was investigated by UV-visible absorption spectra (Fig. 5). From the spectrum of ZnO /PANI composites, the absorption bands of PANI/ZnO nanocomposites showed blue shift which shows decrease in conjugation as a result of interaction between PANI and ZnO The absorbance ratio of benzenoid (π-π transition) to quinoid (polaron- π transition) bands can be taken as a measure of oxidation state of PANI type conducting polymer [Singla *et al*. 2007; Xu *et al*., 2007]. Compared with the UV-visible absorption spectra of nanocomposites, NC1 composite have the highest absorbance ratio of quinoid to benzenoid due to high doping levels. As seen in the UV-visible absorption spectra of PANI and PANI/ZnO nanocomposites, most doped nanocomposite is NC1 that the nanoparticles concentration is highest. This result is in accordance with the results of FTIR spectra.

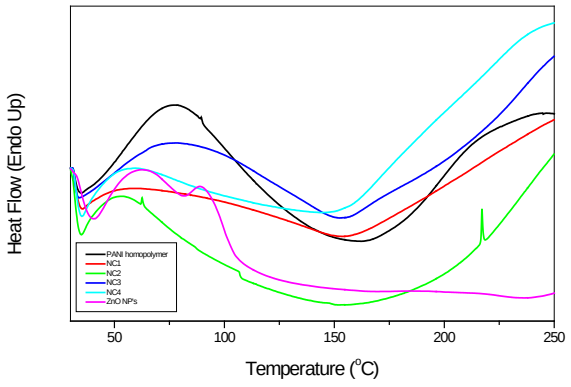

Figure 6. DSC curves of PANI homopolymer, PANI/ZnO nanocomposites and ZnO nanoparticles.

Thermal properties and interaction between the polymers and nanoparticles can also be investigated from the differential scanning calorimetry (DSC) studies. DSC plots showed some endothermic and exothermic peaks for removal of different materials, crystalline melting, recrystallization and polymer decomposition. In order to understand the effect of ZnO nanoparticles on the thermal behaviors of PANI, DSC analysis has been also studied. Fig. 6 shows DSC thermogram of ZnO, PANI and PANI/ZnO composites with various molar ratios of PANI/ZnO. ZnO does not show any endothermic/ exothermic peaks, indicating that there are no physical changes in the sample. It can be seen from DSC curve, two exothermic peaks are observed for PANI. The first peak, with a maximum at ~75°C, is due to the expulsion of water/moisture and the second peak, observed ~240°C, and might be due to thermal degradation of the polymer [Sharma *et al*., 2009c]. In, the DSC curves of PANI/ZnO composites, no exothermic peak is observed clearly. With the incorporation of ZnO, the appearance of the peaks decreased with increasing ZnO concentration as a result of increasing the thermal stability of PANI/ZnO composites with increase ZnO nanoparticles content. NC1 has the highest thermal stability that the nanoparticles concentration is highest.

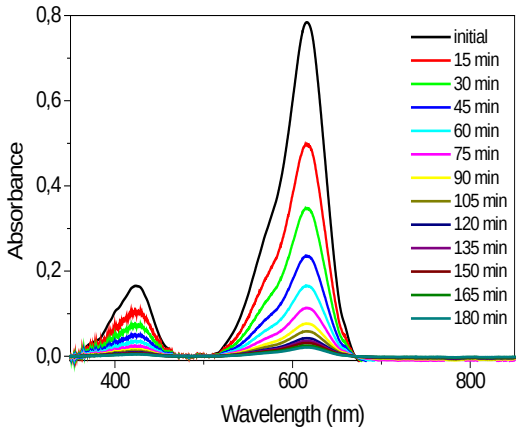

(a)

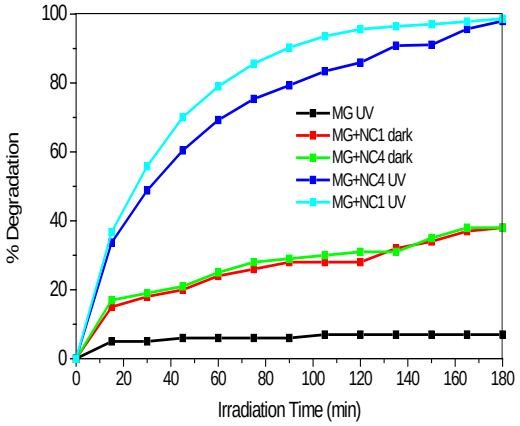

(b)

Figure 7 a) UV-vis absorption spectra of MG dye in the presence of PANI/ZnO nanocomposites for different exposure times under UV light irradiation of MB
b) Extend of decomposition of the MB and MG dyes with respect to time intervals over PANI/ZnO nanocomposite UV light irradiation of MG (Catalyst concentration: 0.4 mg/mL; initial concentration of dyes:1.10 $^{-5}$M) (Catalyst concentration: 1.2 mg/mL; initial concentration of dyes:1.10 $^{-6}$ M)

The absorption spectra of MG in the presence of the NC1 and NC4 under the irradiation of the UV light for various durations can be seen in Fig. 7a. The absorption peaks corresponding to MG at 423 nm and 616 nm, diminished gradually. No new absorption bands appear in either the visible or ultraviolet regions, which indicates the complete photodegradation of MG. Figure 7b shows the variation in decolorizing efficiency versus irradiation time for the MG solutions for the presence of the NC1 and NC4. In order to investigate the effect of irradiation on the PANI/ZnO nanocomposite/dye interaction, three sets of experiments were carried out. The first set involves the degradation of the dyes in the presence of UV light without catalyst. No significant changes were observed in absorption spectrum of dyes, the decolorization efficiency of MG is less than 5% after 180 minutes irradiation under UV light. The results showed that the photolysis of the MG is negligible. In the second set, the experiments were also realized in dark condition to understand the effect of the light source when the catalyst material added into the dye. As can be seen in Fig. 7b, the decolorization efficiencies are 38% for MG dye under dark conditions in the presence of the PANI/ZnO nanocomposites used as catalyst due to adsorption mechanism. The third set of experiments was performed to study the effect of UV light irradiation on the PANI/ZnO nanocomposite /dye interaction. The decolorization efficiencies of the dyes are very higher than corresponding dark conditions in the presence of the PANI/ZnO nanocomposite under illumination. The result indicates that the prepared PANI/ZnO nanocomposites are good catalyst to remove organic pollutants under UV light irradiation.

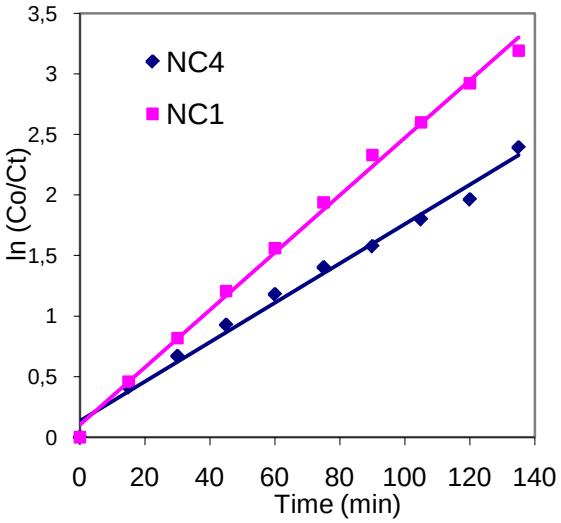

Figure 8. Comparison of the apparent rate constants of MG dye in the presence of NC1 and NC4 nanocomposite photocatalysts under UV light irradiation

In general, the kinetics of photocatalytic degradation of organic pollutants on the semiconducting oxide has been established and can be described well by the apparent first order reaction $\ln(C_0/C_t)=k_{app}.t$, where k_{app} is the apparent rate constant, C_0 is the concentrations of dyes after darkness adsorption for 30 min and C_t is the concentration of dyes at time t. Fig. 8 shows the relationship between illumination time and the degradation rate of MG for UV light illumination. The linear correlation of the plots of $\ln(C_0/C_t)$ versus time suggested a pseudo

first-order reaction for the MG dyes. The apparent rate constants (k_{app}) were determined as 0.0237 min-1 and 0.0162 min-1for NC1 and NC4, respectively. The photocatalytic activity of NC1 is higher than that of NC4 due to the high ZnO content.

5. CONCLUSIONS

PANI/ZnO nanocomposites were successfully synthesized by seeding with ZnO nanoparticles and oxidative polymerization of the aniline monomer in a simple process. We carried out the experiments using different amount of ZnO nanoparticles and maintaining the other reaction conditions unchanged. The SEM study of PANI–ZnO composite film revealed uniform distribution of ZnO nanoparticles in PANI matrix. The absorption peaks in FTIR spectra of PANI–ZnO composite film were found to shift to higher wavenumbers as compared to those observed in pure PANI. The observed shifts were attributed to the interaction between the ZnO nanoparticles and PANI molecular chains. The thermal stability of PANI/ZnO composites is higher than the thermal stability of PANI. The thermal stability of PANI/ZnO composites increased with the increasing of the amount of the ZnO nanoparticles in the reaction mixture. The composite materials were formed from strong interaction between the polymer and ZnO nanoparticles. The nanocomposites synthesized in this study have high efficiency in the degradation of MG under UV light irradiation.

ACKOWLEDGEMENT

The authors are grateful for financial support by the administrative Units of The Research Projects of Selçuk University (project no SUBAP-09101054)

6. REFERENCES

Ameen, S.,. Akhtar, M. S, Kim, Y. S., Yang, O., Shin, H., 2011, "An Effective Nanocomposite of Polyaniline and ZnO: Preparation, Characterizations, and Its Photocatalytic Activity", *Colloid Polym. Sci*., Vol. 289, pp. 415-421.

Bae, H. S., Yoon, M. H., Kim, J. H., Im, S., 2003, "Photodetecting Properties of ZnO-Based Thin-Film Transistors", *Appl. Phys. Lett*., Vol. 83, pp. 5313-5315.

Banerjee, D., Rybczynski, J., Huang, J. Y., Wang, D. Z., Kempa, K., Ren, Z. F., 2005, "Large Hexagonal Arrays of Aligned ZnO Nanorods", *Appl. Phys. A*, Vol. 80, pp. 749-752.

Beek, B. W. J. E., Slooff, L. H., Wienk, M. N., Kroon, J. M., Janseen, R. A. J., 2005, "Hybrid Solar Cells Using a Zinc Oxide Precursor and a Conjugated Polymer", *Adv. Funct. Mater*., Vol. 15, pp. 1703-1707.

Chang, M., Cao, X. L., Zeng, H., Zhang, L., 2004, "Enhancement of the Ultraviolet Emission of ZnO Nanostructures by Polyaniline Modification", *Chem. Phys. Letters*, Vol. 446, pp. 370 -373.

Cho, S., Ma, J., Kim, Y., Sun, Y., Wong, G. K. L., Ketterson, J. B., 1999, "Photoluminescence and Ultraviolet Lasing of Polycrystalline ZnO Thin Films Prepared by the Oxidation of the Metallic Zn", *Appl. Phys. Lett*., Vol. 75, pp. 2761-2763.

Eskizeybek, V., Demir, O., Avcı, A., Chhowalla, M. J., 2011, "Synthesis and Characterization of Cadmium Hydroxide Nanowires by Arc Discharge Method in De-ionized Water", *Nanoparticle Research*, Vol. 13,pp. 4673-4680.

Gangopadhyay, R., De A., 2000, "Conducting Polymer Nanocomposites: A Brief Overview", *Chem. Mater*., Vol 12, pp. 608-622.

Gustafsson, G., Cao, Y., Treacy, G. M., Klavetter, F., Colaneri, N., Heeger, A., 1992, "Flexible Light-Emitting Diodes Made From Soluble Conducting Polymers", *Nature*, Vol. 357, pp. 477-479.

He, Y., 2004, "Preparation of Polyaniline/Nano-ZnO Composites via a novel pickering emulsion route", *Powder Technology*, Vol.147, pp. 59-63.

He, Y., 2005, "A Novel Emulsion Route to Sub-Micrometer Polyaniline/Nano-ZnO Composite Fibers" *App. Surface Sci*., Vol. 249, pp. 1-6.

Khan, A. A, Khalid, M., 2010, "Synthesis of Nano-Sized ZnO and Polyaniline-Zinc Oxide Composite: Characterization, Stability in terms of DC Electrical Conductivity Retention and Application In Ammonia Vapor Detection", *J. App. Polymer Science*, Vol. 117, pp. 1601–1607.

Lee, K., Wu, Z., Chen, Z., Ren, F., Pearton, S. J., Rinzler, A. G., 2004, "Single Wall Carbon Nanotubes for P-Type Ohmic Contacts to GaN Light-Emitting Diodes", *Nano Lett*., Vol. 4, pp. 911-914.

Olson, D. C., Piris, J., Colins, R.T., Shaheen, S. E., Ginley, D. S., 2006, "Hybrid Photovoltaic Devices of Polymer and ZnO Nanofiber Composites", *Thin Solid Films*, Vol. 496, pp. 26-29.

Özgür, Ü., Alivov, Y. I., Liu, C., Teke, A., Reshchikov, M. A., Doğan, S., Avrutin,V., Cho, S. J., Morkoç, H., 2005, "A Comprehensive Review of ZnO Materials and Devices", *Journal of Applied Physics*, Vol. 98, pp. 041301-041403.

Park, W. I., Kim, J. S., Jung, S. W., Yi, G. C, 2002, "Metalorganic Vapor-Phase Epitaxial Growth of Vertically Well-Aligned ZnO Nanorods", *Appl. Phys. Lett*., Vol. 80, pp. 4232-4234.

Paul, G. K., Bhaumik, A., Patra, A. S., Bera, S. K., 2007, "Enhanced Photo-Electric Response of ZnO/Polyaniline Layer-by-Layer Self-Assembled Films", *Mater. Chem. and Phys*., Vol. 106, pp.360-363.

Pouget, J. P., Hsu, C. H., MacDiarmid, A. G., Epstein, A. J., 1995, "Structural Investigation of Metallic PAN-CSA and Some of Its Derivatives", *Synthetic Metals*, Vol. 69, pp. 119-120.

Sailor, M. J., Ginsburg, E. J., Gorman, C. B., Kumar, A., Grubbs, R. H., Lewis, N. S., 1990, "Thin Films of n-Si/Poly-(CH3)3Si-Cyclooctatetraene: Conducting-Polymer Solar Cells and Layered Structures", *Science*, Vol. 249, pp. 1146-1149.

Sharm, S. P., Suryanarayana, M. V. S., Nigam, A. K., Chauhan, A. S., Tomar, L. N. S., 2009, "[PANI/ZnO] Composite: Catalyst for Solvent-Free Selective Oxidation of Sulfides", *Catalysis Communications*, Vol. 10, pp. 905-912.

Sharma, B. K., Gupta, A. K., Dhawan, S. K., Gupta, H. C., 2009, "Synthesis and Characterization of Polyaniline–ZnO Composite and Its Dielectric Behavior", *Synthetic Metals*, Vol. 159, pp. 391-395.

Sharma, B. K., Khare, N., Dhawan, S. K., Gupta, H. C., 2009, "Dielectric Properties of Nano ZnO-Polyaniline Composite in the Microwave Frequency Range", *J. Alloys and Comp*., Vol. 477, pp. 370-373.

Singla, M. L., Sajeela, A., Srivastava, A., Jain, D. V. S., 2007, "Effect of Doping of Organic and Inorganic Acids on Polyaniline/Mn_3O_4 Composite for NTC and Conductivity Behaviour", *Sensors and Actuators A*, Vol.136, pp. 604-612.

Sui, X. M., Shao, C. L., Liu, Y. C., 2005, "White-Light Emission of Polyvinylalcohol/ZnO Hybrid Nanofibers Prepared by Electrospinning", *Appl. Phys. Lett*., Vol. 87, pp. 113-115.

Wang, X., Li, Y., Zhao, Y., Liu, J., Saide, T., Feng, W., 2010, "Synthesis of PANI Nanostructures with Various Morphologies from Fibers to Micromats to Disks Doped with Salicylic Acid", *Synthetic Metals*, Vol. 160, pp 2008-2014).

Wang, X., Summers, C. J., Wang, Z. L., 2005 "Self-attraction among Aligned Au/ZnO Nanorods under Electron Beam", *Appl. Phys. Lett*., Vol.86, pp. 013111-2.

Xu, Z. X., Roy, V. A. L., Stallinga, P., Muccini, M., Toffanin, S., Xiang, H. F., Che, C. M., 2007, "Nanocomposite Field Effect Transistors based on Zinc Oxide/Polymer Blends", *Appl. Phys. Lett*., Vol. 90, pp. 223509-223511.

Yan, Y., Zhang, S. B., Pantelides, S. T., 2001, "Control of Doping by Impurity Chemical Potentials: Predictions for p-Type ZnO", *Phys. Rev. Lett*., Vol. 86, pp. 5723-5726.

Yang, R., Wang, Z. L., 2005, "Interpenetrative and Transverse Growth Process of Self-Catalyzed ZnO Nanorods", *Solid State Commun.*, Vol.134, pp.741-745.

Zamferiscu, M., Kavokin, A., Gil B., Malpuech, G., Kaliteevski, M., 2002, "ZnO as a Material Mostly Adapted for the Realization of Room-Temperature Polariton Lasers", *Phys. Rev. B*, Vol. 65, pp. 161205-161208.

Zhang, M., Fang, S. L., Zakhidov, A. A., Lee, S. B., Aliev, A. E., Williams, C. D., Atkinson, K. R., Baughman, R. H., 2004, "Strong, Transparent, Multifunctional, Carbon Nanotube Sheets", *Science*, Vol. 309, pp. 1215-1219 (2004).